



Improvements of GNSS/INS Localization's Integrity with Gaussian Mixture Filters in a Bayesian Framework

Pierre Sendorek, Karim Abed-Meraim, Maurice Charbit, Sebastien Legoll

► To cite this version:

Pierre Sendorek, Karim Abed-Meraim, Maurice Charbit, Sebastien Legoll. Improvements of GNSS/INS Localization's Integrity with Gaussian Mixture Filters in a Bayesian Framework. The 6th European Workshop on GNSS Signals and Signal Processing, Dec 2013, Munich, Germany. hal-01002195

HAL Id: hal-01002195

<https://hal.science/hal-01002195>

Submitted on 13 Jan 2015

HAL is a multi-disciplinary open access archive for the deposit and dissemination of scientific research documents, whether they are published or not. The documents may come from teaching and research institutions in France or abroad, or from public or private research centers.

L'archive ouverte pluridisciplinaire **HAL**, est destinée au dépôt et à la diffusion de documents scientifiques de niveau recherche, publiés ou non, émanant des établissements d'enseignement et de recherche français ou étrangers, des laboratoires publics ou privés.

Improvements of GNSS/INS localization's integrity with Gaussian Mixture Filters in a Bayesian Framework

Pierre Sendorek, Karim Abed Meraim, Maurice Charbit, Sébastien Legoll

November 6, 2013

Abstract

Gaussian mixture filters model the evolution of the probability density function, *inter alia*, when the noise on the linear measurements is a gaussian mixture. Such a model is relevant when the measurements are subject to disturbances whose statistics may vary abruptly, like the GNSS signals in avionics, which are subject to reflections, scintillation, multipath... The naturally resulting probability density of the hidden state given the observations up to the current time is also a Gaussian mixture, and thus many computations of interest can be done by using well known numerical routines. In particular, it enables to use an algorithm which aims at estimating a position such as its associated protection levels are the smallest (such as the radius of the confidence ball is the smallest). Also, since the number of components of the gaussian mixture grows exponentially with time, we use an algorithm to approximate the probability density at each step by a fixed amount of gaussians. This algorithm iteratively merges the components which result in the smallest changes according to a Kullback-Leibler based metric. Finally, we assess this algorithm that approximates the optimal filter by comparing the empirical integrity (obtained through simulations) to the targeted integrity. We also compare this algorithm with a least squares state of the art estimator by measuring the ratio of their protection levels.

1 Introduction

Gaussian mixture filters (GMF) model the evolution of the probability density function (PDF) when the noise on the linear measurements is a gaussian mixture (GM). This model appears, *inter alia*, when the parameters of the gaussian measurements depend on discrete hidden state variables [Pervan et al., 1998, Pesonen, 2011]. For our GNSS/INS hybridization, the measurements use GPS/Galileo pseudo ranges, GPS/Galileo carrier phase, gyrometer and accelerometer increments. The hidden state discrete variables represent the presence of multipaths, scintillation, ionospheric perturbations. The model we use is relevant when the GNSS signals are subject to disturbances whose statistics may vary abruptly (but not on the same way for the different hidden states). GMF filtering equations handle this case under a bayesian framework and have a theoretical formula which can be expressed with a finite number of usual numerical functions. The drawback is that these equations aren't usable under their exact form since the number of components of the GM grows exponentially with time. Various methods have been developed to reduce the number of components [Runnalls, 2007, Attias, 2000, Bruneau et al., 2010, Pesonen and Piche, 2012]. We adapt the algorithm in [Runnalls, 2007], that iteratively merges the pairs of components of the GM which lead to the smallest changes of the probability density - according to a Kullback-Liebler divergence based metric. But in our case, since the filtering algorithm simultaneously keeps track of several GM - one GM conditionally to each hidden state - we adapt it so as to limit the global number of components instead of limiting the number of components per hidden state. As a result, the allocation of the global number of components is done in function of the complexities of each GM associated to a hidden state. To this end, the allocation is done iteratively, and at each step the components to merge are chosen in the GM for the hidden state in which the minimum change can be achieved. The combination of both the GMF filter and this modified version of algorithm [Runnalls, 2007] yields an approximation of the PDF of the true position given the measurements at each time step, but doesn't yield any estimation of the position.

In avionics the criteria of interest are the protection levels, which are describing the dimensions of a cylinder centered on the estimated position and ensuring to contain the true position with a targeted probability. Thus, instead of using the mean of this PDF as a position estimator, which is well known to minimize the average quadratic error, we use the algorithm [Sendorek et al., 2013] which instead aims at minimizing the size of the protection levels while ensuring a given integrity level. The algorithm in [Sendorek et al., 2013] takes the PDF of the true position as input and yields an estimate of the position, without modifying the PDF. This estimate is thus such as the associated protection levels are minimized. Its purpose is to allow more levels of operation by having protection levels lower than the alert limit fixed by the requirements [DO229, 2006].

The algorithm in [Sendorek et al., 2013] deals in general with a N-dimensional Gaussian mixture and is under the form of a steepest descent which optimizes the position of the center of a ball such as its radius decreases

at each step but still ensures that the sphere centered on the optimized position contains the true position with the targeted probability. After convergence, the obtained solution is thus locally optimal, however, the results in [Sendorek et al., 2013] suggest that the solution is globally optimal. The position yield by this algorithm is computed as being the center of the smallest ball containing a targeted probability to be obtained by the algorithm. Finally, the presented GMF algorithm approximates a theoretically optimal bayesian algorithm which would keep all the components of the GM.

To assess its performance, we measure the empirical integrity and compare it to the targeted integrity. Previous works on GMF defined the estimate of the position as the mean of the gaussian mixture [Pesonen, 2011], which has a closed form expression in our case. We also assess our algorithm by measuring the improvement in terms of protection levels achieved with the estimator defined by algorithm [Sendorek et al., 2013] compared to the mean as defined in [Pesonen, 2011] in presence of disturbances (multipath,...).

The simulations evaluate the performance of our algorithm in function of the global number of components, of the ratios between the covariances of the noises and the probability of occurrence of the outages. The evaluations are performed by simulating a GNSS/INS hybridization with the associated observation and propagation matrices, where the discrete hidden states modelize the probability of a multipath and where the covariance and the mean of the noise for each hidden state modelize the possible threats.

This paper starts by presenting the protection levels in section 2, which are the criteria of integrity of the estimators in avionics. Then, in section 3 we introduce the model of propagation and observation of the state vector. Section 4 presents the filtering equations. We describe the principle of the algorithm used to reduce the number of components in the GM in section 5. Section 6 briefly introduces the mecanization equations used to make our simulations, and further describes some parameters of the model. The experimental protocol and evaluation results will be found in 7

2 Protection Levels

A common measure of integrity of a position estimator \hat{X} are the protection levels. The protection levels are dimensions describing a cylinder in the 3-dimensional space that ensures to contain the estimated position with given probabilities, for any possible disturbance. However in our case, for the purpose of our study, we restrict the possible disturbances to be the one described by the statistical model from section 3. The cylinder is tangent to the local WGS84 ECEF [ce ne serait pas plutôt NED ?] horizontal plane and is described by the horizontal protection level (HPL or horizontal protection radius) and the vertical protection level (VPL or vertical protection radius). The VPL is a value such that the difference between the altitudes of the true position and the estimated position is smaller than the VPL with a probability of $1 - \alpha_{\text{req}}^{\text{V}}$. Similarly, the HPL is a value such that the true position's horizontal coordinates lie in a disc centered on the estimated position, of radius HPL and with a probability of $1 - \alpha_{\text{req}}^{\text{H}}$, where $\alpha_{\text{req}}^{\text{V}}$ and $\alpha_{\text{req}}^{\text{H}}$ are values derived from the avionics' requirements [DO229, 2006]. Our study focuses on the VPL for which the equations in algorithm [Sendorek et al., 2013] can be computed without using the Monte-Carlo methods but thanks to ordinary numerical routines and thus be used with a greater accuracy and speed. The VPL must satisfy these constraints for any possible disturbance. Rigorously, if we call P_V the projector on the vertical ECEF axis, the VPL for a position estimator \hat{X} is a value of the radius r belonging to the set

$$\mathcal{R} = \left\{ r \in \mathbb{R}^+, \mathbb{P} \left(\|P_V(\hat{X} - X)\| \leq r \right) \geq 1 - \alpha_{\text{req}}^{\text{V}} \right\}$$

This definition of the protection levels is thus adapted to our context where all the possible disturbances are supposed to be described by the model from section 3.

3 Model

Assume the propagation and observation model is given by

$$X_{t+1} = F_t \cdot X_t + U_t$$

$$Z_t = H_t \cdot X_t + E_{J_t} \cdot B_{J_t} + V_t$$

with the difference, compared to the usual Gaussian model, that J_t is a hidden discrete variable indicating which disturbance (multipath, scintillation, ionospheric perturbations) affects the observation, and where

- X_t is the continuous part of the state vector containing, among other values, the error on the position, inertial measurements errors but also satellite noises (which have a Markovian behaviour). In the following we call X_t the continous part of the state vector (in contrast to J_t) which is a Gaussian process satisfying $X_{t+1} = F_t \cdot X_t + U_t$, where F_t is a known linear matrix and $U_t \sim \mathcal{N}(0, C_U)$, with a known covariance matrix. We call Q_t the associated transition kernel which satisfies $Q_t(x_{t+1}|x_t) = f_{X_{t+1}|X_t}(x_{t+1}|x_t)$.

- $Z_t \in \mathbb{R}^{N_{\text{sat}}}$ is the pseudo ranges vector at time t . It contains the GNSS measurements of the problem linearized around a position close to the receiver.
- H_t is the (known) observation matrix at time t . This matrix is not assumed to be full rank. A multiplication of X_t by this matrix has for effect to sum multiply the position errors of X_t by a geometry matrix and to add the time correlated errors of X_t

$$H_t.X_t = \left[\begin{array}{c|c|c} G_t & 0 & I \end{array} \right] \cdot \left[\begin{array}{c} \text{position error components of } X_t \\ \text{other components of } X_t \\ \text{time correlated satellite's noise of } X_t \end{array} \right]$$

where G_t is the so called cosine matrix at time t (see [Kaplan and Hegarty, , Parkinson and Spilker, 1996]).

- $V_t \sim \mathcal{N}(0, C_V)$. V_t is independent from $V_{t'}$ for $t' \neq t$. It's values will be described in section 6.
- As already mentioned J_t is a hidden discrete random variable. In the following we will call it the discrete part of the state vector. To encompass a broader amount of cases, we assume that J_t follows a Markov chain with the transition matrix $q(j_{t+1}|j_t) = \mathbb{P}(J_{t+1} = j_{t+1}|J_t = j_t)$. In most of the cases this transition matrix will be chosen close to identity, to express the fact that if the signal enters in a state (multipath, scintillation, ionospheric perturbations), it has tendency to stay in this state for some amount of time. It's value can be derived from average time of staying in a state and from the frequency of switching from one state to another. For the purpose of illustrating how our algorithm works, we will assume that J_t is a set containing the satellites (which are indexed by integers in $\{1, \dots, N_{\text{sat}}\}$) subject to reflections. This variable is modelled as a hidden state variable because of its Markovian behaviour.
- $E_{J_t} = (e_i)_{i \in J_t}$ is a matrix formed by stacking the canonical line vectors $e_i = (0, \dots, 0, 1, 0, \dots, 0)$ for $i \in J_t$ being the number of the satellite in J_t . If $J_t = \emptyset$ then $E_{J_t} = 0$.
- B_{J_t} is a column vector which has for length the cardinality of J_t . We assume that in our case it follows δ_0 when $J_t = \emptyset$ and otherwise it follows $\mathcal{N}(\phi_{J_t}, S_{J_t})$. This law describes the behaviour of the signal when there is a presence of multipath, scintillation, or ionospheric disturbance depending on the value of J_t .

4 Filtering Equations

Filtering equations associated to the model described in section 3 have a closed form expression (and their computation can be done at each step thanks to a finite amount of calls to ordinary mathematical functions). In this section the equations are derived from the well known filtering equations. For sake of readability, we denote by $Y_t = (X_t, J_t)$ the whole hidden state vector. The filtering equations (see [Arulampalam et al., , Cappé et al., 2005]) are thus

$$f(y_{t+1}|z_{0:t+1}) \propto f(z_{t+1}|y_{t+1}) \int f(y_{t+1}|y_t) f(y_t|z_{0:t}) dy_t$$

Which is written modulo a multiplicative constant, that can be obtained by ensuring that $f(y_{t+1}|z_{0:t+1})$ sums to 1 when summing on all possible values of y_{t+1} . Note that $\int f(y_{t+1}|y_t) f(y_t|z_{0:t}) dy_t = f(y_{t+1}|z_{0:t})$ is the probability density of the “propagated” hidden state vector. The update consists in the multiplication of this density by $f(z_{t+1}|y_{t+1})$ (followed by a normalization, implicit here). By developing this equation in our case, since the states of the pseudo-ranges $(J_t)_t$ and the continuous state vector $(X_t)_t$ are mutually independent sequences, we get

$$f(x_{t+1}, j_{t+1}|z_{0:t+1}) \propto f(z_{t+1}|x_{t+1}, j_{t+1}) \sum_{j_t \in \mathcal{J}} q(j_{t+1}|j_t) \cdot Q(x_{t+1}|x_t) \cdot f(x_t, j_t|z_{0:t}) \cdot dx_t$$

Assuming that $f(x_0|j_0, z_0)$ is a gaussian, with this model, it is easy to see that $f(x_t, j_t|z_{0:t})$ is a GM for each $t > 0$ and for each value of $j_t \in \mathcal{J}$, thanks to the decomposition

$$f(x_t|j_t, z_{0:t}) = \sum_{j_{0:t-1} \in \mathcal{J}^t} f(x_t|z_{0:t}, j_{0:t}) f(j_{0:t}|z_{0:t})$$

In this decomposition, the states $j_{0:t}$ are given, and $f(x_t|z_{0:t}, j_{0:t})$ is a gaussian PDF, since the conditioning implies that the transformations are linear. Note that it can be obtained thanks to the ordinary Kalman equations [Pesonen and Piche, 2012] with the assumption that the initial state $f(x_0|j_0, z_0)$ is gaussian. Hence, since $j_{0:t} \in \mathcal{J}^{t+1}$ is a discrete variable, $f(x_t, j_t|z_{0:t})$ is a GM. This model fits into the definition of a Conditionally Gaussian Linear State Space Model (CGLSSM) as described in [Cappé et al., 2005]. Although this formula is explanatory, it lacks of a development that would allow a recursive implementation, therefore we will develop the filtering equations in the next section.

4.1 Propagation

We express the effect of the propagation of the continuous part of the state vector, X_t , thanks to the inertial measurements, for any given value of j_t . This value can be computed without exhibiting the expression of Q but only by using the fact that the propagation sums up to a linear transform followed by the addition of a gaussian noise.

$$\int Q(x_{t+1}|x_t) \cdot f(x_t, j_t | z_{0:t}) \cdot dx_t = \sum_{i=1}^{N_{\text{gauss}}(j_t)} w_{(j_t, i)} \mathcal{N}(x_t; F_t \cdot \mu_{(j_t, i)}, F_t \cdot C_{(j_t, i)} \cdot F_t^T + C_U)$$

The propagation of the whole state vector is obtained by taking in account the transitions between the discrete states

$$f(x_{t+1}, j_{t+1} | z_{0:t}) = \sum_{j_t \in \mathcal{J}} q(j_{t+1} | j_t) \sum_{i=1}^{N_{\text{gauss}}(j_t)} w_{(j_t, i)} \mathcal{N}(x_t; F_t \cdot \mu_{(j_t, i)}, F_t \cdot C_{(j_t, i)} \cdot F_t^T + C_U)$$

For each j_{t+1} , this probability is thus expressed as a linear combination of probabilities under the form of a GM. It is thus also a GM. We express it in a simpler way with generic notations as

$$f(x_{t+1}, j_{t+1} | z_{0:t}) = \sum_{i=1}^{N_{\text{gauss}}(j_{t+1})} w_{(j_{t+1}, i)} \mathcal{N}(x_{t+1}; \mu_{(j_{t+1}, i)}, C_{(j_{t+1}, i)})$$

4.2 Observation term

The update is accounted by multiplying the propagated density by the likelihood of the propagated state

$$f(z_{t+1} | x_{t+1}, j_{t+1}) = \mathcal{N}(z_{t+1}; H_{t+1} \cdot x_{t+1} + E_{j_{t+1}} \cdot \phi_{j_{t+1}}, E_{j_{t+1}} \cdot S_{j_t} \cdot E_{j_{t+1}}^T + C_V)$$

which can be rewritten as $= \gamma \cdot \exp \left\{ -\frac{1}{2} \|x_{t+1} - m\|_S^2 \right\}$ (1)

where $\gamma = \frac{|\Gamma|^{\frac{1}{2}}}{\sqrt{2\pi}^{\dim(z)}} \exp \left\{ -\frac{1}{2} \|(I - P)(E - z)\|_\Gamma^2 \right\}$, with $\Gamma = (E_{j_{t+1}} \cdot S_{j_t} \cdot E_{j_{t+1}}^T + C_V)^{-1}$ and $P = H(\Gamma^{\frac{1}{2}} H)^\dagger \Gamma^{\frac{1}{2}}$ which is the orthogonal projector on $\text{Im}(H)$ related to the norm $\|\cdot\|_\Gamma$ (see appendix 9.1). The precision matrix is $S = H^T \Gamma H$ and the mean $m = (\Gamma^{\frac{1}{2}} H)^\dagger \Gamma^{\frac{1}{2}} (z - E)$. We denote by $H = H_{t+1}$, $E = E_{j_{t+1}} \cdot \phi_{j_{t+1}}$. The pseudo inversion used here is the general pseudo inversion (for a system which is both overdetermined and underdetermined).

4.3 Update by the observation

First, note that if we denote by $\hat{X} = (C^{-1} + S)^{-1}(C^{-1}\mu + Sm)$ we can rewrite

$$\|x - \mu\|_{C^{-1}}^2 + \|x - m\|_S^2 = \|x - \hat{X}\|_{(C^{-1}+S)}^2 - \|\hat{X}\|_{(C^{-1}+S)}^2 + \|\mu\|_{C^{-1}}^2 + \|m\|_S^2$$

We can remark that S is only a positive semi definite matrix since H_{t+1} is not a full rank matrix, but the sum $C^{-1} + S$ is an invertible matrix since C is positive definite as a covariance matrix. We can note the similarity with Kalman filter's updated state's mean by noticing that

$$\begin{aligned} \hat{X} &= (C^{-1} + S)^{-1}(C^{-1}\mu + Sm) \\ &= \mu - (C^{-1} + S)^{-1}(C^{-1} + S)\mu + (C^{-1} + S)^{-1}(C^{-1}\mu + Sm) \\ &= \mu + (C^{-1} + S)^{-1}S(m - \mu) \end{aligned}$$

Finally we can express the pdf of the state vector given all the observation up to the current time

$$\begin{aligned} f(x_{t+1}, j_{t+1} | z_{0:t+1}) &\propto f(z_{t+1} | x_{t+1}, j_{t+1}) \cdot f(x_{t+1}, j_{t+1} | z_{0:t}) \\ &\propto \gamma_{j_{t+1}} \cdot e^{-\frac{1}{2} \|x_{t+1} - m_{j_{t+1}}\|_{S_{j_{t+1}}}^2} \cdot \sum_{i=1}^{N_{\text{gauss}}(j_{t+1})} w_{(j_{t+1}, i)} \mathcal{N}(x_{t+1}; \mu_{(j_{t+1}, i)}, C_{(j_{t+1}, i)}) \\ &\propto \sum_{i=1}^{N_{\text{gauss}}(j_{t+1})} \frac{\gamma_{j_{t+1}} \cdot w_{(j_{t+1}, i)} w'_{(j_{t+1}, i)} |(C_{(j_{t+1}, i)}^{-1} + S_{j_{t+1}})|^{\frac{1}{2}}}{|C_{(j_{t+1}, i)}|^{\frac{1}{2}}} \mathcal{N}\left(x_{t+1}; \hat{X}_{(j_{t+1}, i)}, (C_{(j_{t+1}, i)}^{-1} + S_{j_{t+1}})^{-1}\right) \end{aligned}$$
 (2)

where

$$\log(w'_{(j_{t+1},i)}) = -\frac{1}{2} \|\mu_{(j_{t+1},i)}\|_{C_{(j_{t+1},i)}^{-1}}^2 - \frac{1}{2} \|m_{j_{t+1}}\|_{S_{j_{t+1}}}^2 + \frac{1}{2} \|\hat{X}_{(j_{t+1},i)}\|_{(C_{(j_{t+1},i)}^{-1} + S_{j_{t+1}})}^2$$

and similarly

$$\hat{X}_{(j_{t+1},i)} = (C_{(j_{t+1},i)}^{-1} + S_{j_{t+1}})^{-1} (C_{(j_{t+1},i)}^{-1} \mu_{(j_{t+1},i)} + S_{j_{t+1}} m_{j_{t+1}})$$

Hence we can derive the quantity of interest, the pdf of X_{t+1} given all the observations up to time $t + 1$ by integrating out j_{t+1}

$$f(x_{t+1}|z_{0:t+1}) = \sum_{j_{t+1} \in \mathcal{J}} f(x_{t+1}, j_{t+1}|z_{0:t+1})$$

The obtained PDF is a GM again. We use the algorithm described in [Sendorek et al., 2013] which aims to find a position estimation such as the associated protection levels are the tightest. Although the obtained position is not strictly speaking always the one which leads to the tightest protection levels, the associated protection levels yield by this algorithm are the true ones (i.e. the probability that the true position lies outside the confidence interval is exactly α_{req}^V), assuming that the variable in question really follows the GM given in equation 2. In the next sections we denominate by LOB the algorithm described in [Sendorek et al., 2013].

5 Reduction of the number of components

At this stage, after having found an estimate of the position based on a “good” approximation of the PDF (for instance using the LOB algorithm), we perform the necessary reduction of the number of components thanks to a modification of the algorithm [Runnalls, 2007] to bound the computational load for next step. The resulting PDF is thus an approximation of the exact PDF, and of the quality of this approximation depends the exactness of the approximation of the protection levels. The algorithm used to reduce the number of components uses a metric based on the KL distance to measure the loss of information induced by the potential replacement of a pair components by the component which matches their first and second order moments and whose weight is the weight of the pair. If two components are described by their weight, their mean and their covariances $(w_i, \mu_i, C_i)_{i=1,2}$, the component resulting from the merge of both writes (w, μ, C) where the weight is $w = w_1 + w_2$, the mean is $\mu = \frac{w_1}{w_1 + w_2} \cdot \mu_1 + \frac{w_2}{w_1 + w_2} \cdot \mu_2$ and the covariance is $C = \sum_{i \in \{1,2\}} \frac{w_i}{w_1 + w_2} (C_i + (\mu_i - \mu) \cdot (\mu_i - \mu)^T)$. The algorithm iteratively searches for the pair which leads to the smallest loss and replaces it as long as the number of components is too high. The search is done among the set $\left\{ \left(\left(\frac{w_{(j_t,i)}}{\sum_{i'} w_{(j_t,i')}} \right), \mu_{(j_t,i)}, C_{(j_t,i)} \right), \left(\frac{w_{(j_t,k)}}{\sum_{k'} w_{(j_t,k')}} \right), \mu_{(j_t,k)}, C_{(j_t,k)} \right) \right\}, j_t \in \mathcal{J}, i \neq k, (i, k) \in \{1, \dots, N_{\text{gauss}}(j_t)\}^2$, which is the list of pairs of gaussian components describing each GM which approximates $p(x_t|j_t, z_{0:t})$ for all the possible values of j_t . The measure of the loss of information is denoted B and is an upper bound of the KL distance between the mixture of two components and the merged components. Its definition is

$$B[(w_1, \mu_1, C_1), (w_2, \mu_2, C_2)] = \frac{1}{2} [(w_1 + w_2) \log \det(C) - w_1 \log \det(C_1) - w_2 \log \det(C_2)]. \quad (3)$$

The interesting property of this criterion is that the components which are merged have in general close means and similar covariances. It seems thus legitimate to use it to decide which components will be merged, since the global shape of the resulting pdf is in general conserved. In our case, since $p(x_t|j_t, z_{0:t})$ is a GM for each value of j_t , instead of constraining the number of gaussians for each j_t , we constrain the global number of components and let the algorithm choose the number of gaussians needed to represent the GM for each value of j_t . The algorithm rather runs on $p(x_t|j_t, z_{0:t})$ than on $p(x_t, j_t|z_{0:t})$ because the probability to switch between discrete hidden states is likely high in our context of abrupt variations, so at each moment, an observation may abruptly increase the posterior probability of being in a discrete state and the probability density of the corresponding continuous state has to be a good approximation as soon as the switch occurs.

6 Mecanization

Our filter monitors the errors of estimation around a linearization point as in [Titterton and Weston, 2004]. The continuous state vector contains the attitude errors expressed in the local NED coordinates, respectively denoted by $(\delta\phi_N, \delta\phi_E, \delta\phi_D)$, for the north, east, and down axis. The vector X_t also contains the velocity errors $(\delta V_N, \delta V_E, \delta V_Z)$, and the errors on the position $(\delta L, \delta G, \delta h)$, which are respectively the error on the longitude, the error on the latitude and the error on the height. The variation of these values are expressed in function of the gyroscopic drifts $(\delta\omega_N, \delta\omega_E, \delta\omega_D)$, of the earth’s angular momentum Ω_T , of the earth’s radius R_T , of the gravitational constant g , of the errors on the accelerometric biases $(\delta b_{acc,N}, \delta b_{acc,E}, \delta b_{acc,Z})$ and of the velocities (V_N, V_E, V_D) supposed to be constant in our simulations.

6.1 Continuous equations

The discrete mecanization equations are derived from

$$\begin{aligned}
\frac{\partial \delta \phi_N}{\partial t} &= \delta \omega_N - \frac{\delta V_E}{R_T} + \Omega_T \sin(L) \delta L + \frac{V_N}{R_T} \delta \phi_Z - \left(\frac{V_E}{R_T} \tan(L) + \Omega_T \sin(L) \right) \delta \phi_E \\
\frac{\partial \delta \phi_E}{\partial t} &= \delta \omega_E + \frac{\delta V_N}{R_T} + \left(\frac{V_E}{R_T} + \Omega_T \cos(L) \right) \delta \phi_Z + \left(\frac{V_E}{R_T} \tan(L) + \Omega_T \sin(L) \right) \delta \phi_N \\
\frac{\partial \delta \phi_Z}{\partial t} &= \delta \omega_D + \frac{\delta V_E}{R_T} \tan(L) + \left[\frac{V_E}{R_T} (1 + \tan^2(L)) + \Omega_T \cos(L) \right] \delta L - \frac{V_N}{R_T} \delta \phi_N - \left(\frac{V_E}{R_T} + \Omega_T \cos(L) \right) \delta \phi_E \\
\frac{\partial \delta V_N}{\partial t} &= \delta b_{\text{acc},N} - g \cdot \delta \phi_E \\
\frac{\partial \delta V_E}{\partial t} &= \delta b_{\text{acc},E} + g \cdot \delta \phi_N \\
\frac{\partial V_Z}{\partial t} &= \delta b_{\text{acc},Z} + [2\Omega_T \sin(L) V_E] \delta L \\
\frac{\partial \delta L}{\partial t} &= \frac{\delta V_N}{R_T} \\
\frac{\partial \delta G}{\partial t} &= \frac{\delta V_E}{R_T \cos(L)} + \frac{V_E \sin(L)}{R_T \cos^2(L)} \delta L \\
\frac{\partial \delta h}{\partial t} &= -\delta V_Z
\end{aligned}$$

Ideally, the accelerometer bias and the gyrometer drift would be constant if there was no propagation noise, thus we add those two lines

$$\begin{aligned}
\frac{\partial \delta b_{\text{acc},N}}{\delta t} &= \frac{\partial \delta b_{\text{acc},E}}{\delta t} = \frac{\partial \delta b_{\text{acc},Z}}{\delta t} = 0 \\
\frac{\partial \delta \phi_N}{\delta t} &= \frac{\partial \delta \phi_E}{\delta t} = \frac{\partial \delta \phi_Z}{\delta t} = 0
\end{aligned}$$

6.2 Discrete equations

From these equations is derived the propagation matrix F_t . The discretization is made for a timestep $\Delta t = 1s$. The previous equations give a relation of the form $\frac{\partial \tilde{X}(t)}{\partial t} = A \cdot \tilde{X}(t)$ where A is a linear function and \tilde{X} is a vector only containing the states described in previous section, hence the discretization scheme we use is $\tilde{X}_{t+1} = I + \Delta t \cdot A \cdot \tilde{X}_t$. The full continous state vector X_t contains the states in \tilde{X}_t but also contains the previous states of the GNSS signals, multiplied by $e^{-\frac{\Delta t}{\tau}}$ to modelize their $\tau = 30 \times 60s$ time correlation. The propagation matrix F_t is in our case a block matrix, where the upper part relates to the propagation of the vector \tilde{X} and the lower part relates to the propagation of the GNSS pseudo ranges

$$F_t = \left[\begin{array}{c|c} I + \Delta t \cdot A & 0 \\ \hline 0 & e^{-\frac{\Delta t}{\tau}} I \end{array} \right]$$

The time-decorrelated part of the measurement noise C_V is a diagonal matrix and the corresponding variances are, with obvious notations

- $\sigma_{\delta \phi_N}^2 = \sigma_{\delta \phi_E}^2 = \sigma_{\delta \phi_Z}^2 = 1.4 \times 10^{-4} \text{rad}^2$
- $\sigma_{\delta V_N}^2 = \sigma_{\delta V_E}^2 = \sigma_{\delta V_Z}^2 = 2 \times 10^1 (m/s)^2$
- $\sigma_{\delta L}^2 = 4 \times 10^{-10} \text{rad}^2$
- $\sigma_{\delta G}^2 = 6 \times 10^{-10} \text{rad}^2$
- $\sigma_{\delta h}^2 = 1.5 \times 10^4 m^2$
- $\sigma_{\delta w_N}^2 = \sigma_{\delta w_E}^2 = \sigma_{\delta w_D}^2 = 10^{-10} \text{rad}^2$

- $\sigma_{\delta b_{acc,N}}^2 = \sigma_{\delta b_{acc,E}}^2 = \sigma_{\delta b_{acc,D}}^2 = 10^{-5} \text{rad}^2$

where the last two lines model the evolution of the accelerometers biases and of the gyrometers drifts.

The covariance matrix also contains the variances of the time-correlated pseudo range noise $\sigma_{\text{pseudo-range}}^2 = (1 - e^{-\frac{2\Delta t}{\tau}}) \times 15^2 m^2$, which is the same for each pseudo range. This value ensures that the standard deviation of the stationary law of each the pseudo-range is $15m$.

Finally, the time decorrelated part of the noise, C_V , is taken equal to $5^2 Im^2$.

7 Evaluation

7.1 Protocol

We compare the results yield by the LOB to the results yield by the bayesian least square estimator as defined in [Pesonen, 2011] which we will denominate by ℓ_2 in this paper. Both estimators base their estimation on the PDF yield by the modified version of the algorithm [Runnalls, 2007] described in section 5. For both estimators, we compare the targeted integrity to the empirical integrity for the vertical axis as follows. A sequence of hidden states $(X_t, J_t)_{t=0:T}$ is drawn according to the model described in section 3. From this sequence of hidden states is drawn a sequence of observations $Z_{0:T}$. Both filters are run with the same sequence of observations as input. At each time step, each of both filters predicts a position on the vertical axis and its associated $(1 - \alpha)$ confidence interval (where we note for short $\alpha = \alpha_{\text{req}}^V$). To assess the quality of this confidence interval, we measure the number of times when the true position is outside of the confidence interval and divide it by T . Without any reduction of the number of components, this proportion would tend to exactly α . We also measure the gain in terms of the size of the protection levels between both estimators.

Simulations are performed for various sets of parameters $(n_{\text{gauss}}, \beta, \sigma_B^2)$, where n_{gauss} determines the average number of gaussians tracked per hidden state. In our case $N_{\text{sat}} = 4$ hence the number of hidden states is $N_{\text{sat}} + 1 = 5$ under the assumption of at most one possible reflection for all the GNSS signals. The bound on the total number of gaussians is thus $5n_{\text{gauss}}$. The parameter β determines the transition between the discrete hidden states in the Markov Chain. The 5×5 transition matrix is $q = (1 - \beta)I + \frac{\beta}{N_{\text{sat}}}(\mathbb{I} - I)$, where \mathbb{I} is a matrix full of ones. The parameter σ_B^2 determines the covariance matrix of the disturbance, such as $B_{J_t} \sim \mathcal{N}(0, \sigma_B^2)$ if $J_t \neq \emptyset$ and $B_{J_t} \sim \delta_0$ if $J_t = \emptyset$. The simulations are made for every $\alpha \in \{10^{-1}, 10^{-2}, 10^{-3}, 10^{-4}\}$ and for every possible element $(n_{\text{gauss}}, \beta, \sigma_B^2) \in \{2, 6\} \times \{1, 1/3\} \times \{30^2, 120^2\}$. The sets of parameters used in the simulations are denoted by roman numbers and the corresponding parameters are given in table 1

	I	II	III	IV	V	VI	VII	VIII
σ_B^2	30^2	120^2	30^2	120^2	30^2	120^2	30^2	120^2
n_{gauss}	6	6	2	2	6	6	2	2
β	1	1	1	1	$\frac{1}{3}$	$\frac{1}{3}$	$\frac{1}{3}$	$\frac{1}{3}$

Table 1: Correspondence between the roman numbers and the parameters

7.2 Results

	$\alpha = 10^{-1}$	10^{-2}	10^{-3}	10^{-4}
I	1.3α	1.9α	2.8α	5.0α
II	0.9α	0.9α	1.5α	1.2α
III	1.4α	1.9α	2.2α	5.0α
IV	2.0α	3.1α	3.4α	6.2α
V	1.2α	1.4α	1.2α	1.2α
VI	1.0α	1.0α	0.8α	1.2α
VII	1.2α	1.4α	1.2α	1.2α
VIII	1.0α	1.0α	0.8α	2.5α

Table 2: Complementary to one of the empirical integrity for the LOB algorithm

	$\alpha = 10^{-1}$	10^{-2}	10^{-3}	10^{-4}
I	1.3α	2.1α	3.1α	6.2α
II	0.9α	1.0α	1.5α	1.2α
III	1.4α	2.0α	2.6α	3.8α
IV	2.0α	3.0α	3.5α	5.0α
V	1.2α	1.5α	1.5α	2.5α
VI	1.0α	1.0α	0.9α	2.5α
VII	1.2α	1.4α	1.6α	2.5α
VIII	1.0α	1.0α	0.9α	2.5α

Table 3: Complementary to one of the empirical integrity for the ℓ_2 algorithm

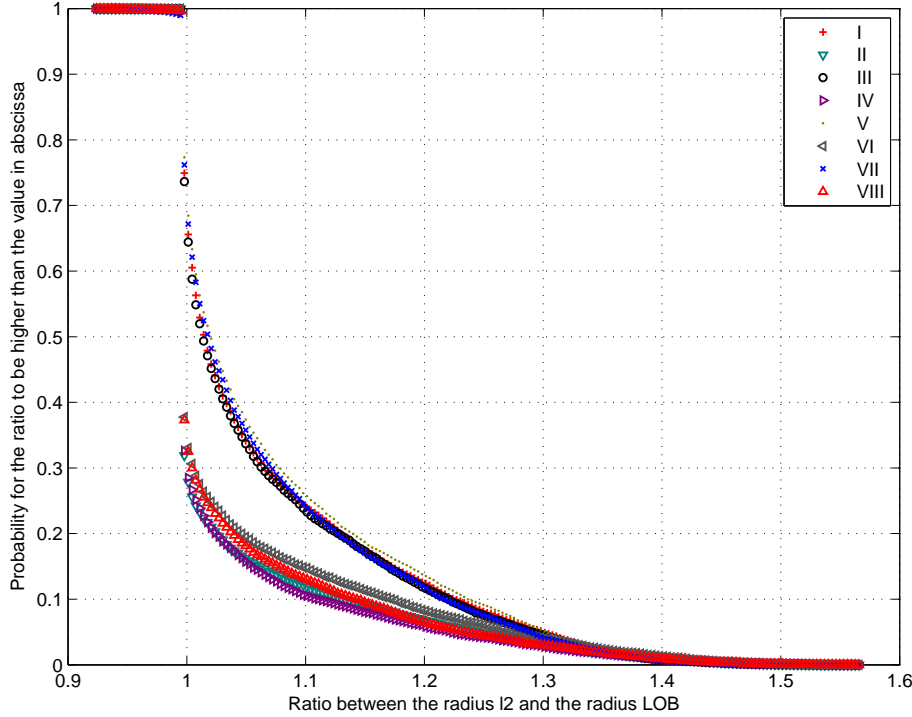


Figure 1: Empirical complementary cumulative function of the ratios of the vertical protection levels for $\alpha = 10^{-3}$

Tables 2 and 3 show that in our simulations, the empirical integrity achieved with this method is in general close to the targeted integrity. The first obvious remark is that when $n_{\text{gauss}} = 6$ the results are closer to the targeted integrity than when $n_{\text{gauss}} = 2$: the algorithm reaches an integrity closer to the targeted one when the approximation of the true PDF is better. Also, the empirical integrity is closer to the targeted integrity when the noise σ_B^2 is big. The reason for this is partly due to the fact that a noise with a big variance is easily identified, hence the corresponding discrete state's probability is strongly reduced. Thus the PDF described by the GM is close to a single gaussian PDF, and the GM reduction algorithm doesn't make too much approximation by merging the gaussians with a low probability (which are more likely to be merged according to the formula 3 of B). Less obvious is the fact that the filter reaches an integrity close to the targeted integrity when the probability of switching between the discrete states is lower. Part of the reason for this is that when the probability of switching between states is small, the current state is more accurately identified thanks to previous measurements. Thus, for the filter there is less ambiguity concerning the value of current hidden discrete state and thus concerning the sources to take into account to give the best estimation of the continuous state vector. These results are particularly interesting when the probabilities of switching from a discrete state to another are low.

Figure 1 gives a comparison of the empirical ratios of the ℓ_2 and the LOB estimators. In general for all our simulations, the LOB yields radiuses 10% smaller than the ℓ_2 in more than 10% of the cases. The improvement obtained with the LOB are more significant when the noise is $\sigma_B^2 = 30^2 m^2$. This noise is big enough to have a non negligible impact on the position estimation, but is too small for the LOB to estimate the underlying state with a good confidence. Thus the PDF is a sum of non overlapping gaussians and the ℓ_2 estimator is affected by components of the GM which have a small weight but which are outlying whereas the LOB estimator is more robust in this case and provides a radius smaller by 20% in more than 10% of the cases.

8 Perspectives

The method used to reduce the number of gaussians described in section 5 doesn't aim at preserving the global similarity with the initial PDF. The similarity is iteratively maximized between the pair of components to be replaced and their first and second order moment matching gaussian, but it is unclear if there is an advantage of using this strategy regarding the goal of preserving a global similarity. Furthermore, another point which is not clear is the impact of the choice of a KL distance based similarity regarding the criterion of the protection levels. This choice is rather motivated by the ease of use of the formula due to its links with Information Theory that established some useful properties and interpretations of the involved quantities. In this context, Variational Bayes methods [Bruneau et al., 2010, Attias, 2000, Pesonen and Piche, 2012] may provide some more robust solutions to preserve a

global approximation.

Another perspective of improvement would be to reduce the GM basing on the measurements from future timesteps. These measurements would help to decrease the weight of improbable failure states and thus enable to make a better choice concerning the components to merge. In fact, we hope that measurements from the future could “disambiguate” the current hidden state, in the sense that the distribution $f(x_t|j_t, z_{0:t+N})$ would be closer to a single Gaussian pdf. Since the measurements from the future are not available, for a practical implementation, the reduction of the GM would rather be done a few steps in the past on $f(x_{t-N}|j_{t-N}, z_{0:t})$. Then, the density $f(x_t|j_t, z_{0:t})$ would have to be computed on the basis of $f(x_{t-N}|j_{t-N}, z_{0:t})$.

9 Appendix

9.1 Projector relative to a norm

Let $\|\cdot\|_A$ be a norm. We define the projection matrix on $Im(H)$ with respect to this norm by reducing the problem to the ordinary norm $\|\cdot\| = \|\cdot\|_I$. The problem is thus to find x such as $\|Hx - m\|_A^2$ is minimal. We have

$$\|Hx - m\|_A^2 = \|A^{\frac{1}{2}}(Hx - m)\|^2 = \|A^{\frac{1}{2}}Hx - A^{\frac{1}{2}}m\|^2$$

This norm is minimized for $x = (A^{\frac{1}{2}}H)^{\dagger}A^{\frac{1}{2}}m$. The orthogonal projector on the image of H with respect to the norm $\|\cdot\|_A$ thus writes $H(A^{\frac{1}{2}}H)^{\dagger}A^{\frac{1}{2}}$.

References

- [Arulampalam et al.,] Arulampalam, S., Maskell, S., and Clapp, T. A tutorial on particle filters for online nonlinear/non-gaussian bayesian tracking. University of Cambridge.
- [Attias, 2000] Attias, H. (2000). A variational bayesian framework for graphical models. *Advances in neural information processing systems*, 12(1-2):209–215.
- [Bruneau et al., 2010] Bruneau, P., Gelgon, M., and Picarougne, F. (2010). Parsimonious reduction of gaussian mixture models with a variational-bayes approach. *Pattern Recognition*, 43(3):850–858.
- [Cappé et al., 2005] Cappé, O., Moulines, E., and Rydén, T. (2005). *Inference in hidden Markov models*. Springer.
- [DO229, 2006] DO229 (2006). *Minimum Operational Performance Standards for Global Positioning System/Wide Area Augmentation System Airborne Equipment*. 1828 L Street, NW, Suite 805, Washington, D.C. 20036 USA.
- [Kaplan and Hegarty,] Kaplan, E. D. and Hegarty, C. J. *Understanding GPS, Principles and Applications, second edition*. Artech House.
- [Parkinson and Spilker, 1996] Parkinson, B. W. and Spilker, J. J. J. (1996). *Global Positioning System Theory and Applications*, volume 1. American Institute of Aeronautics and Astronautics.
- [Pervan et al., 1998] Pervan, B. S., Pullen, S. P., and Christie, J. R. (1998). A multiple hypothesis approach to satellite navigation integrity. *Navigation*, 45(1):61–71.
- [Pesonen, 2011] Pesonen, H. (2011). A framework for bayesian receiver autonomous integrity monitoring in urban navigation. *Navigation*, 58(3):229–240.
- [Pesonen and Piche, 2012] Pesonen, H. and Piche, R. (2012). Estimation of linear systems with abrupt changes of the noise covariances using variational bayes algorithm. *Tampereen teknillinen yliopisto. Matematiikan laitos. Tutkimusraportti-Tampere University of Technology. Department of Mathematics. Research Report; 100*.
- [Runnalls, 2007] Runnalls, A. R. (2007). Kullback-leibler approach to gaussian mixture reduction. *Aerospace and Electronic Systems, IEEE Transactions on*, 43(3):989–999.
- [Sendorek et al., 2013] Sendorek, P., Abed Meraim, K., Charbit, M., and Legoll, S. (2013). Locally optimal confidence ball for a gaussian mixture random variable. *Indoor Positioning and Indoor Localization 2013 - To be published*.
- [Titterton and Weston, 2004] Titterton, D. and Weston, J. (2004). *Strapdown Inertial Navigation Technology*. The American Institute of Aeronautics and Astronautics, second edition.